Peer-reviewed version available at Int. J. Mol. Sci. 2018, 19, 1393; doi:10.3390/ijms19051393

Article

New Insight into the Octamer of TYMS stabilized by Intermolecular Cys43-disulfide

Dan Xie [1,a], Lulu Wang [2,a], Qi Xiao [1], Xiaoyan Wu [1], Lin Zhang [1], Qingkai Yang [1,*] and Lina Wang [1,*]

[1] Institute of Cancer Stem Cell, DaLian Medical University, 9 Western Lvshun South Road, Dalian, Liaoning 116044, China;
[2] School of Life Science and Biotechnology, Dalian University of Technology, No 2 Linggong Road, Dalian, Liaoning 116024, China;
[a] Dan Xie and Lulu Wang contributed equally to this work.
[*] **Correspondence author**: Yangqingkai@dlmedu.edu.cn and Linawang1109@hotmail.com

Abstract: Thymidylate synthase (TYMS) is an essential enzyme for the de novo synthesis of dTMP and has been a primary target for cancer chemotherapy. Although the physical structure of TYMS and the molecular mechanisms of TYMS catalyzing the conversion of dUMP to dTMP have been conducted thorough studies, oligomeric structure remains unclear. Here, we show that human TYMS not only exists in dimer but also octamer by intermolecular Cys43-disulfide formation. We optimize the expression condition of recombinant human TYMS using *Escherichia coli* system. Using HPLC-MS/MS, we show that purified TYMS has catalytic activity for producing dTMP. In the absence of reductant β-mercaptoethanol, SDS-PAGE and size exclusion chromatography (SEC) showed size of TYMS protein is about 35 KDa, 70 KDa, and 280 KDa. While the Cys43 was mutated to Gly, the band of ~280 KDa and the peak of octamer disappeared. Therefore, TYMS was determined to form octamer, dependent on the presence of Cys43-disulfide. By measuring Steady-State Parameters for monomer, dimer and octamer, we found the k_{cat} of octamer is increased slightly than monomer. On the basis of these findings, we suggest that octamer in the active state might have a potential influence on the design of new drug targets.

Keywords: thymidylate synthase (TYMS); monomer; dimer; octamer; overexpression and purification

1. Introduction

Classical thymidylate synthase (TYMS), encoded by the thyA gene, is highly conserved in most eukaryotes, including humans [1, 2]. It catalyzes the transfer of a methylene group from the cofactor 5, 10-methylenetetrahydrofolate (mTHF) to its substrate deoxyuridine monophosphate (dUMP) and forms deoxythymidine monophosphate (dTMP), yielding dihydrofolate (DHF) as a secondary product [3-5]. A second class of thymidylate synthases, flavin-dependent thymidylate synthases (FDTSs) [6-8], is encoded by the thyX gene and has been found primarily in prokaryotes and viruses [6, 9]. FDTSs utilize a noncovalently bound flavin adenine dinucleotide (FAD) prosthetic group to catalyze the redox chemistry and use mTHF only as a methylene donor. Several organisms, including human pathogens, rely solely on thyX for thymidylate synthesis. Recent studies further showed the catalytic mechanism of TYMS and FDTS [2, 10], which are essential enzymes for DNA replication and frequently targeted by chemotherapeutic and antibiotic drugs [11, 12]. However, drug resistance has become an increasing concern due to the long-term use [13-16]. Therefore, researchers continue to search for effective and specific inhibitors of TYMS to overcome resistance problem.

Peer-reviewed version available at *Int. J. Mol. Sci.* **2018**, *19*, 1393; doi:10.3390/ijms19051393

Extensive knowledge of structure and properties of the target protein could contribute to formulating more efficient strategies for drug development. Many studies reported TYMS exists as dimer–monomer equilibrium, whose two residues R175 and R176 form part of the dUMP binding site and the TYMS dimer form can adopt active and inactive conformation [17-19]. There is evidence that the TYMS dimer interface play an important role in TYMS-mRNA recognition, perhaps by controlling a conformational change of the protein that exposes the mRNA binding site [20-22]. In addition, Chu *et al.* thought the dimer obligates catalytic function, while the monomer is believed to play a crucial role in TYMS-mRNA regulation [23]. Whereas these different insights in TYMS structure and function, it is of undeniable importance to further investigate the oligomeric form of TYMS protein, which contributes to design compounds that bind at the oligomer interface of TYMS. Such compounds could overcome drug resistance problems [24].

The aim of this study was to determine the oligomer state of TYMS and reconstitute the dTMP synthesis system in vitro. We optimized the overexpression condition of TYMS, such as the host strain, the inducer concentration, temperature and culture medium. TYMS catalytic activity for producing dTMP was assessed by mass spectrometry method. More importantly, we use SDS-PAGE and size exclusion chromatography (SEC) to analyze oligomeric state of TYMS. The data proof full functionality of TYMS on DNA biosynthesis and show that TYMS coexist in octamer–dimer–monomer equilibrium and Cys-43 disulfide contribute to octamer formation. In conclusion, our study demonstrate that octamer exists as active state by measuring steady-state parameters of different oligomeric form.

2. Results

2.1. TYMS overexpression and purification

To optimize the overexpression condition of target protein, five different E.*coli* strains (Tuner (DE3), BL21 (DE3), C41 (DE3), C43 (DE3), and BL21 (DE3)-pLysS) and bacteria concentrations of adding IPTG were used to screen initially. The results show that 0.8 OD_{600} is the optimal for pLysS (Figure. S1A), C43 (Figure. S1B), and C41 (Figure. S1C), while 0.6 OD_{600} is the optimal for BL21 (Figure. S1D) and Tuner (Figure. S1E). Then, compared with all the expression level of the optimal bacterial density of different strains, we found 0.8 OD_{600} for pLysS is the optimal expression level (Figure. S1F). Additionally, the concentration of isopropyl-β-d-thiogalactoside (IPTG), the temperature and four different types of media were also screened. The optimal induction condition for TYMS was found to be 0.4 mM IPTG and LB medium at 20 °C, after the cells reaching 0.8 OD_{600} for pLysS (Figure. S1G, H, and I). Hence, we chose the recombinant 0.4 mM IPTG-LB-20°C-0.8OD_{600}-pLysS for large-scale expression condition.

After confirming the optimal system, overexpressed TYMS was examined with western blot and then purified with Nickel column twice. The samples were subjected to SDS-PAGE following by Coomassie brilliant blue staining after incubating at 100°C with loading buffer containing β-mercaptoethanol. Figure. S2A shows enrichment of TYMS via Ni-NTA chromatography yielded a large amount of full-length protein. After the protein was purified twice, they were diluted equivalently, and subjected to SDS-PAGE following by Coomassie Brilliant (Figure. S2B, S2C) to detect the purity of proteins, more than 90%. Finally, according to BSA standard curve (Figure. S2D), the concentration of purified TYMS was determined to be > 60 mg/mL.

2.2. Reconstitution of TYMS-mediated dTMP synthesis

The catalytic mechanism of classical thymidylate synthases is presented in Figure. 1A. To formally test the functionality of such a pathway and to provide a tool to investigate its mechanistic features, we reconstituted the entire process of reductive methylation with defined components. Using dUMP substrate, we performed reductive methylation to measure the formation of dTMP using HPLC-MS/MS. Multiple reaction monitoring (MRM) was used to determine base ion mass transitions of dU (229.1 to 113.1), dT (243.1 to 127.1) (Figure. 1B, 1C). Standard curves were built to quantify dU and dT modification (Figure. 1D, 1E). In the absence of TYMS, no dT was detectable.

Preprints (www.preprints.org) | NOT PEER-REVIEWED | Posted: 2 April 2018 doi:10.20944/preprints201804.0014.v1

Peer-reviewed version available at Int. J. Mol. Sci. 2018, 19, 1393; doi:10.3390/ijms19051393

However, full reconstitution of the TYMS with the dUMP and mTHF substrates generated a substantial amount of dU (Figure. 1F). Together, these results demonstrate that TYMS-mediated reductive methylation of dUMP generates dTMP.

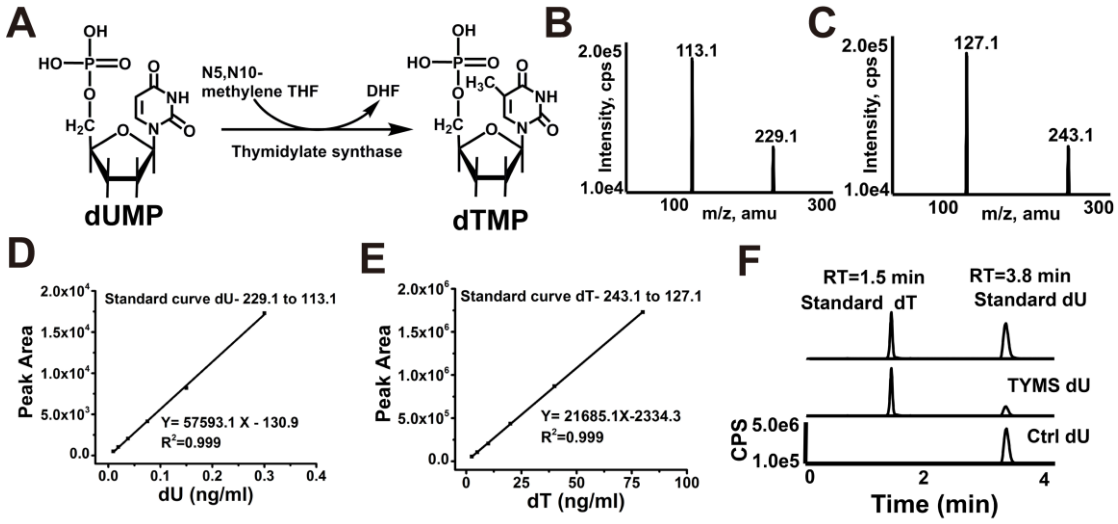

Figure 1. HPLC-MS-MS assay measures the reductive methylation activity of TYMS in vitro. (A) dUMP and mTHF as co-substrate generates dTMP by TYMS, yielding DHF as a secondary product. (B and C) Base ion mass transitions for LC-MS-MS analysis of dU and dT standard. The MRM transitions were monitored as follows: 229.1 to 113.1 (dU); 243.1 to 127.1 (dT). (D and E) LC-MS-MS standards curves of dU and dT. (F) LC-MS-MS profiles of nucleosides derived from TYMS treatment. The upper LC-MS-MS profile shows nucleoside dU and dT standards. The lower LC-MS-MS profile shows dT generation in vitro reaction system of TYMS with dU as substrate.

2.3. TYMS formed octamer by intermolecular Cys43-disulfide

To determine the existence of the homologous dimer, we used Coomassie Brilliant and Western Blot to analyze the status of the TYMS protein. Surprisingly, after TYMS incubating with loading buffer (no β-mercaptoethanol) at 37°C, we found TYMS shows three bands and the molecular weight was ~35 kDa, ~70 kDa, and ~280 kDa, respectively (Figure. 2A, 2B). Compared to the condition at 37°C, after TYMS incubating with loading buffer (no β-mercaptoethanol) at 100°C, the bands of ~70 kDa and ~280 kDa weaken (Figure. 2C, 2D). While TYMS was incubated with loading buffer (containing β-mercaptoethanol) at100°C, the band of ~280 kDa disappeared and the band of ~70 kDa weakens. This phenomenon makes us speculate that TYMS may exist as octamer, and the proportion of each oligomeric form in different conditions were shown in Figure S3. To investigate the active or inactive conformation of TYMS, we incubated TYMS with dUMP and mTHF and subjected to SDS-PAGE following by Western Blot (Figure. 2E) and Coomassie Brilliant (Figure. 2F) subjected. The results showed that the bands of ~70 kDa and~280 kDa remain unchanged, compared to samples without dUMP and mTHF. This suggested octamer of TYMS is in the active state.

To further investigate the oligomer form of TYMS, we performed a calibration SEC experiment with five protein standards, including myosin (212.0 kDa), beta-galactosidase (116.0 kDa), bovine serum albumin (67.0 kDa), ovalbumin (43.0 kDa), and ribonuclease A (13.7 kDa). The established standard curve allowed a more reliable estimation of the protein molecular weight for the SEC column. As shown in the Figure. 2G, the lg (Mr) value is plotted as a function of the retention volume. The experimental standard curve was well fitted by the equation $y=3.4823-0.0472x$ with $R^2= 0.998$. TYMS (6 mg/mL) was subjected to SEC and collected at a retention volume of 22.25 mL, 33.83mL and 41.5 ml (Figure. 2H). Meanwhile, TYMS (3 mg/mL) was subjected to SEC in the presence or absence of dUMP and mTHF (Figure 2I, 2J). The results indicated that the octamer is independent on the concentration and substrates of TYMS. And then, the collected sample was subjected to Western Blot and Coomassie Brilliant (Monomer was detected with SDS-PAGE while dimer and octamer with

NATIVE-PAGE.) (Figure. 2K). According to the standard curve equation and western blot marker, the molecular weight of TYMS was estimated to be ~35 kDa, ~70 kDa, and ~280 kDa, which was about twice and eightfold as much as the theoretical molecular weight of monomeric TYMS (35 kDa), indicating that the TYMS protein existed oligomeric forms as dimmer, and octamer by intermolecular Cys-disulfide.

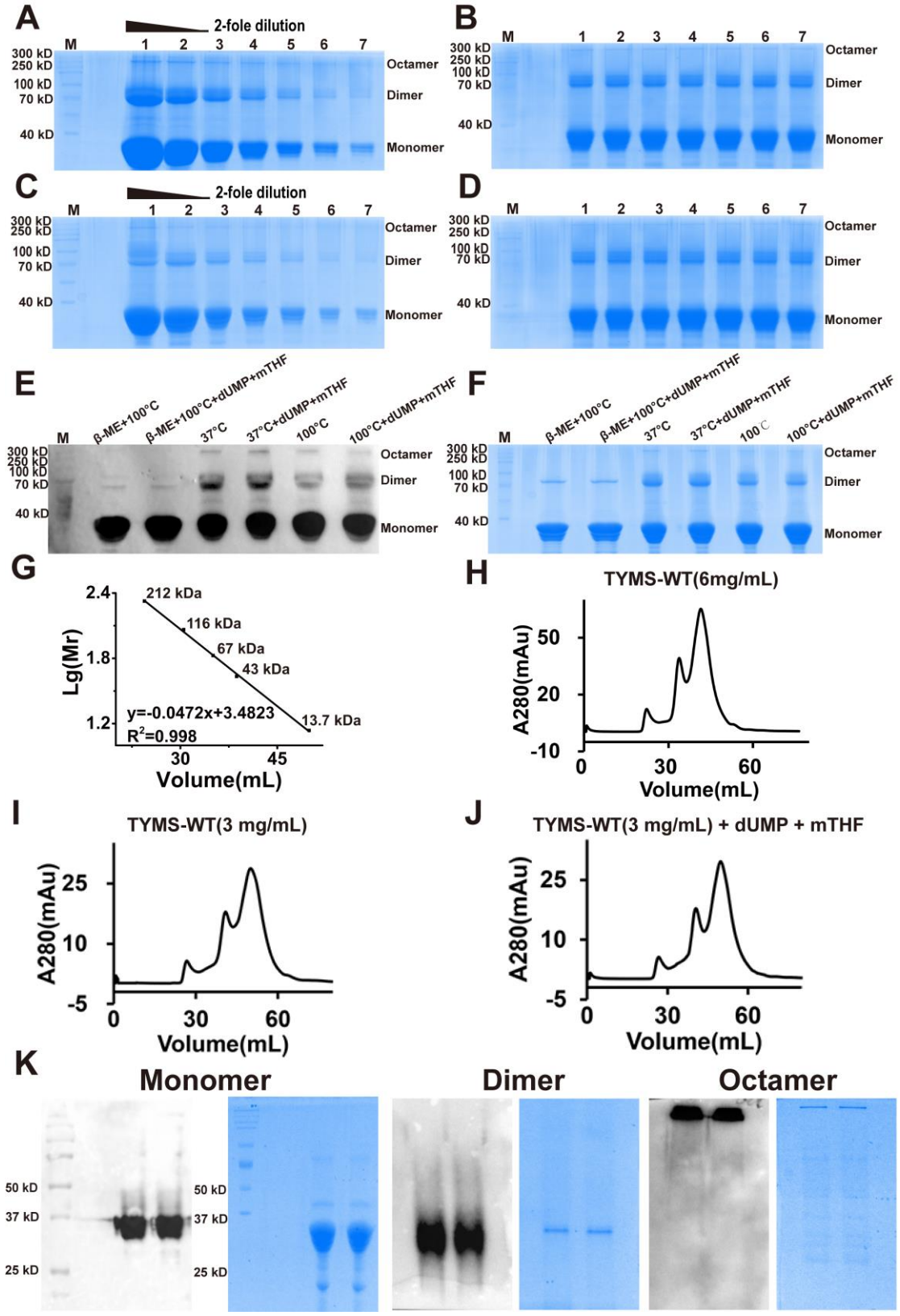

Figure 2. The determination of protein dimers and octamers. (A) Coomassie Brilliant of concentrated proteins incubated without β-mercaptoethanol (β-ME) for 10 min at 37°C: 1) undilutedly concentrated proteins; 2) double diluted proteins; 3) four times diluted proteins; 4) eight times diluted proteins; 5) sixteen times diluted proteins; 6) thirty-two times diluted proteins; 7) sixty-four times diluted proteins. The MW of monomer, dimer and octamer are ~35kDa, ~70kDa, ~280kDa respectively. (B) Coomassie Brilliant of eight diluted proteins incubated without β-mercaptoethanol (β-ME) for 10 min at 37°C. (C) Coomassie Brilliant of concentrated proteins incubated without β-mercaptoethanol (β-ME) for 10 min at 100°C: 1) undilutedly concentrated proteins; 2) double diluted proteins; 3) four times diluted proteins; 4) eight times diluted proteins; 5) sixteen times diluted proteins; 6) thirty-two times diluted proteins; 7) sixty-four times diluted proteins. (D) Coomassie Brilliant of eight times diluted proteins incubated without mercaptoethanol for 10 min at 100°C. (E)Western Blot and (F) Coomassie Brilliant: 1) TYMS was directly incubated with loading buffer (containing β-mercaptoethanol) for 10 min at 100°C; 2) TYMS reacting with dUMP and mTHF for 1 h at 37°C, and then incubated with loading buffer (containing β-mercaptoethanol) for 10 min at 100°C; 3) TYMS was directly incubated with loading buffer (without β-mercaptoethanol) for 10 min at 37°C; 4) TYMS reacting with dUMP and mTHF for 1 h at 37°C, and then incubated loading buffer (without β-mercaptoethanol) 10 min in 37°C; 5) TYMS was directly incubated with loading buffer (without β-mercaptoethanol) for 10 min at 100°C; 6) TYMS reacting with dUMP and mTHF for 1 h at 37°C, and then incubated loading buffer (without β-mercaptoethanol) for 10 min at 100°C. (G) Standard curve for molecular weight estimation and (H) Size exclusion chromatography. Peak 1, 2, 3 represent a symmetrical peak eluted at a retention volume of ~22.25 mL, ~33.83 mL, ~41.5 mL, indicating that TYMS existed in octamer, dimeric, and monomer form. (I) Size exclusion chromatography that protein was diluted to 3 mg/mL. (J) Size exclusion chromatography that protein was diluted to 3 mg/mL with dUMP and mTHF. (K) The western blot and Coomassie Brilliant of component separated by SEC. The monomer was subjected to SDS-PAGE, while dimer and octamer were subjected to NATIVE-PAGE.

To determine which Cys site is contribute to the form of octamer, we examined the effect of Cys43, Cys180 and Cys210 disulfide on the TYMS octamer by mutating these to Gly (Depicted as red in Figure 3A), due to the Cys195 as active site and Cys199 contributed to dimerization interface [5, 25, 26]. TYMS (Cys43Gly), TYMS (Cys180Gly) and TYMS (Cys210Gly) were expressed and purified with Ni-NTA chromatography twice, and then they were detected by Western Blot (Figure 3B), Coomassie Brilliant without β-mercaptoethanol (Figure. 3C) and SEC (Figure 3D). The band of octamer ~280 kDa and the peak at 22.25 mL in TYMS (Cys43Gly) has disappeared while there were no changes in TYMS (Cys180Gly) and TYMS (Cys210Gly), which demonstrate Cys43 residue is essential for octamer.

Preprints (www.preprints.org) | NOT PEER-REVIEWED | Posted: 2 April 2018 doi:10.20944/preprints201804.0014.v1

Peer-reviewed version available at Int. J. Mol. Sci. 2018, 19, 1393; doi:10.3390/ijms19051393

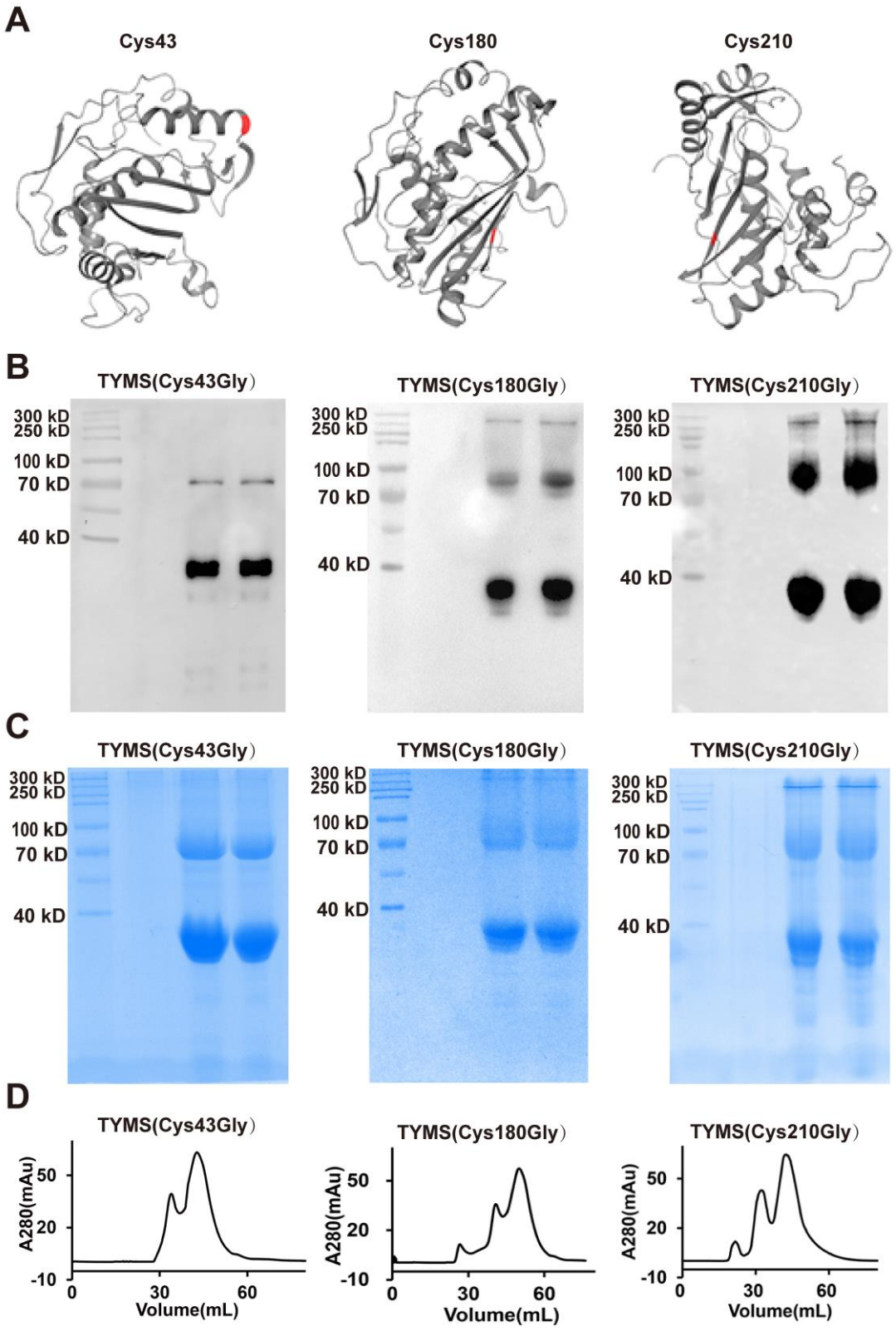

Figure 3. Determination of the oligomeric state of TYMS by mutated Cys. (A) Available TYMS structures of Cys43, Cys180 and Cys210, and the site is depicted as red. The data derived from PDB (Protein Data Bank), and the ID is 1YPV. (B) and (C) Western Blot and Coomassie brilliant of TYMS with Cys43Gly, Cys180Gly or Cys210Gly (without β- mercaptoethanol). (D) Size exclusion chromatography about TYMS with Cys43Gly, Cys180Gly or Cys210Gly.

Preprints (www.preprints.org) | NOT PEER-REVIEWED | Posted: 2 April 2018 doi:10.20944/preprints201804.0014.v1

Peer-reviewed version available at *Int. J. Mol. Sci.* **2018**, *19*, 1393; doi:10.3390/ijms19051393

2.4. Analysis of Kinetic Properties of all Oligomeric Forms

To further analyze the effect of octamer, we detected the Steady-State Parameters of all the Oligomeric Forms by measuring the formation of DHF. The reaction process curves for dUMP and mTHF of monomer, dimer and octamer were shown in Figure 4A-4F, respectively. The K_m values for dUMP were increased by 3-fold for dimer and 1.32-fold for octamer compared with monomer (Figure 4G). The K_m values for mTHF were increased by 2.9-fold for dimer and 1.6-fold for octamer relative to that for monomer (Figure 4H). The V_{max} and k_{cat} values for dUMP of dimer were decreased slightly while the octamer increased than monomer and the same results for mTHF, suggested that the octamer of TYMS is in the active state, which is consistent with the result shown in Figure 3E and 3F. The experimental standard curve of DHF was well fitted by the equation y=0.00394 + 0.00446x with R^2= 0.999 (Figure 4I).

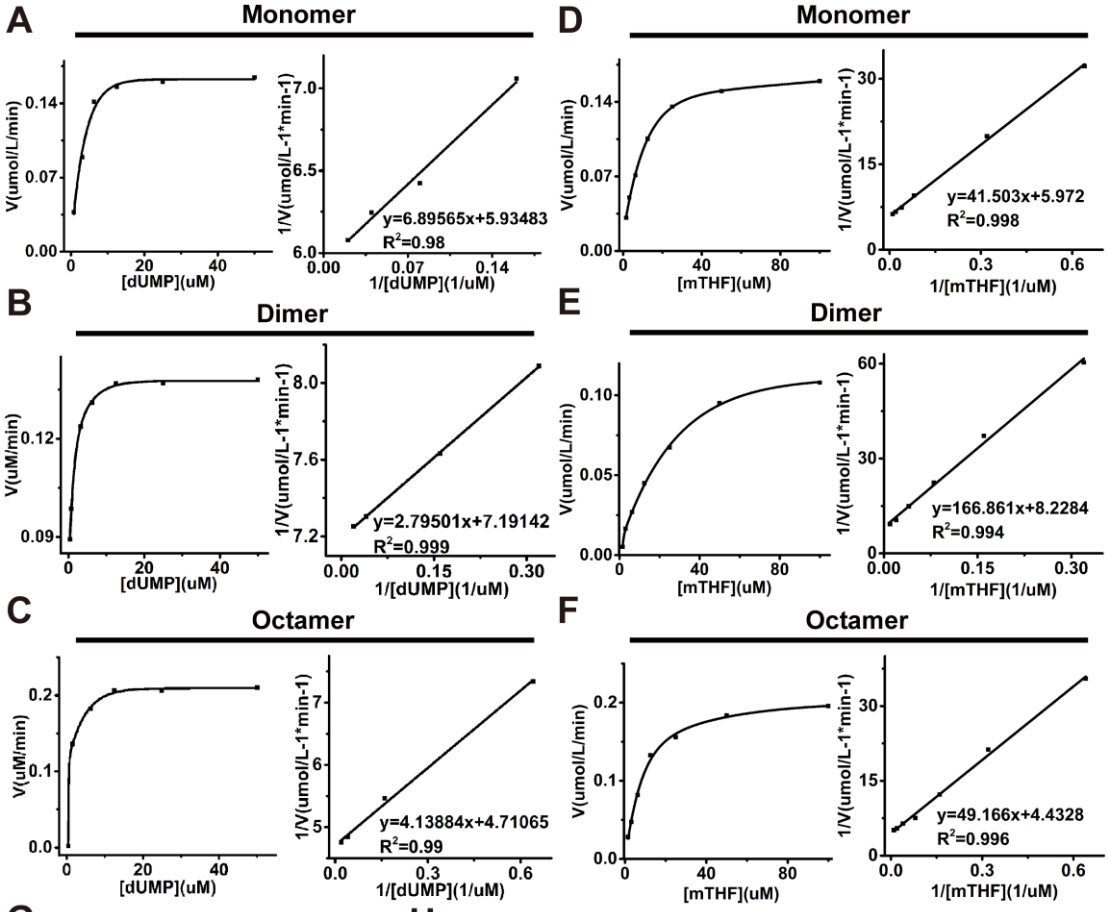

G

dUMP	Monomer	Dimer	Octamer
K_m (uM)	0.861	2.573	1.138
V_{max} (uM/min)	0.168	0.139	0.212
$k_{cat}(s^{-1})$	0.225	0.168	0.283

H

mTHF	Monomer	Dimer	Octamer
K_m (uM)	6.949	20.28	11.09
V_{max} (uM/min)	0.167	0.122	0.226
$k_{cat}(s^{-1})$	0.223	0.163	0.301

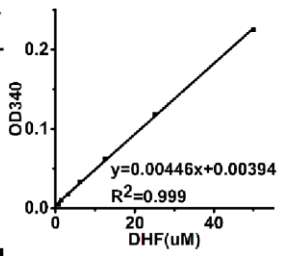

Figure 4. The reaction process curves and Steady-State Parameters for different Oligomeric forms of TYMS. (A) Reaction process curves of dUMP for TYMS monomer, the left panel showed substrate saturation curve, and the right panel showed the Lineweaver–Burk double-reciprocal plot. (B) Reaction process curves of dUMP for TYMS dimer. (C) Reaction process curves of dUMP for TYMS octamer. (D) Reaction process curves of mTHF for TYMS monomer. (E) Reaction process curves of mTHF for TYMS dimer. (F) Reaction process curves of mTHF for TYMS octamer. (G) Steady-State

Parameters of dUMP for different Oligomeric form. (H) Steady-State Parameters of mTHF for different Oligomeric form. (I) Standard curve for Ultraviolet absorption value at OD_{340} of DHF.

3. Discussion

Recent research on the only de novo source of synethsized dTMP points towards a mechanism involving TYMS. Despite the classic of this pathway, experimental evidence that directly links TYMS activity with mTHF and dUMP is insufficient and oligomeric form of TYMS remains unclear. This work aimed to analyze oligomeric form of TYMS and reconstitute TYMS-mediated dTMP synthesis.

In line with spectrophotometric assay [27], our work provides mass spectrum evidence for a direct productive action of TYMS with mTHF and dUMP, confirming dTMP generation (Figure. 1). Reaction efficiency of dUMP to dTMP reaches at least 20%, suggesting the TYMS we purified has enzyme activity. Many studies have reported TYMS exists in the dimer, which has two distinct states: one is the active state in the crystal structures of TYMS-nucleotide-(anti) folate ternary complexes [28]; the other one is an inactive state in sulfate-containing conditions [29]. The cavity in the dimer interface could serve as an allosteric site of to regulate the conformational switching between the active and inactive states [1, 30]. In addition, TYMS performs at least two different functions with specific interaction regions: dimer obligates catalytic function, while both the monomer and dimer are believed to play a crucial role in TYMS-mRNA recognition and regulation [31-34]. In this study, we found TYMS not only formed dimer, but also octamer by intermolecular Cys43-disulfide (Figure 3). Octamer is a higher homologous aggregation and in an active conformation, and the V_{max} and k_{cat} were increased slightly (<1.5-fold) for the octamer while the K_m was decreased (<1.5-fold) (Figure. 3 and Figure 5). To the best of our knowledge, this is the first detailed report on octamer of TYMS in an active conformation. Still, roles of the octamer are unclear. Since dimers have such an important function, it is possible octamer structure of TYMS may potentially affect the activity of TYMS so as to provide new drug targets to overcome resistance problem, and synthesis of other nucleotides so that the appropriate balance of the four nucleotides required for DNA synthesis is maintained. It should be noted that this study only examined molecular weight of TYMS using SDS-PAGE and SEC. Our results are lack of crystallographic data. Despite its preliminary character, this study can clearly indicate TYMS coexists in octamer–dimer–monomer equilibrium.

In summary, this current work serves as the first comprehensive evaluation of oligomer structure and the activities of TYMS in vitro. And provides a foundation for further inquiry into the role of this very interesting DNA synthesis and repair enzyme.

4. Materials and Methods

4.1. Plasmid Construction

The human TYMS (NM_001071.2) sequence is amplified by polymerase chain reaction (PCR) from human cDNA (reverse transcription from total mRNA) with primers (PET28A-TYMS-HindIII-Forward and PET28A-TYMS-XhoI-Reverse). TYMS (Cys43Gly), TYMS (Cys180Gly) and TYMS(Cys210Gly) are amplified by Fusion PCR[35] with primers PET28A-TYMS-HindIII-Forward, TYMS-43-Forward, TYMS-43-Reverse, TYMS-180-Forward, TYMS-180-Reverse, TYMS-210-Forward, TYMS-210-Reverse and PET28A-TYMS-XhoI-Reverse (The sequence of primers were showed in Table S1). The fragments were cloned into the pET-28a (+) vector using the restriction recognition site for Hind III and Xho I, carrying a N-terminal 6× His tag. DNA sequencing was used to verify the sequences of the constructed vector.

4.2. Expression Screening

To find out an optimized expression condition for TYMS, the vector pET-28a-6His-TYMS was transformed into Tuner (DE3), BL21(DE3), C41(DE3), C43 (DE3), BL21 (DE3)-pLysS. When IPTG (MedChemExpress) was added, we optimized bacterial density including 0.3 OD_{600}, 0.5 OD_{600}, 0.8 OD_{600}, 1.1 OD_{600}, 1.3 OD_{600}, for different host strains. Furthermore, for the best host cell and its optional

bacteria concentration, it was cultured in the nutrient-rich medium 32Y and several modified mediums, including LB, 2× TYE and 4× TY (Compositions of culture media were shown in Table S2) [36]. And then, the appropriate concentration of IPTG containing 0.1 mM, 0.2 mM, 0.4 mM and 0.8 mM was investigated. Finally, the inducing temperature was optimized at 20°C, 25°C, and 30°C.

4.3. Protein purification

Cells were harvested by centrifugation at 5000× g for 10 min at 4°C and washed twice with ice-cold PBS. And then, 2 g cell pellets were suspended with 10 mL of PBS which contains 1 mM $MgCl_2$, 10 mM imidazole (MedChemExpress), and protease inhibitor cocktail, and DNase at final concentrations of 1 mM, 20 mM, 1 mg/mL, 1 tablet/50 mL, and 100 U/mL, respectively. Resuspended cells were broken through Ultrasonic Cell Disruptor (NOISE ISOLATING CHAMBER JY 92-IIN) on the ice, on 5 s off 5 s. Lysed cells were subjected to centrifugation at 100,000×g for 1 h at 4°C to obtain the supernatant. The supernatant containing TYMS was then loaded onto a Ni-NTA column pre-equilibrated with binding buffer (PBS buffer, 150 mM NaCl,10% (v/v) glycerol, 20 mM imidazole, pH7.4). The resins were then washed 8 times with the binding buffer containing 20 mM imidazole to remove non-specifically bound proteins, and bound protein was eluted with elution buffer (PBS buffer, 150 mM NaCl,10% (v/v) glycerol,400 mM imidazole, pH7.4). To obtain more purified TYMS, we purify this protein twice using Ni-NTA column as described above. Purified TYMS was concentrated using an Amicon Ultrafree centrifugal filter (Millipore Corporation, Billerica, MA, USA) with a cutoff of 10 kDa. The concentration buffer contains 20 mM Tris-Base, 150 mM NaCl and 10% (*v*/*v*) glycerol at pH7.4. Protein concentration was determined using the BCA assay according to manufacturer's instructions (Pierce, Rockland, IL, USA). (Components of buffers are shown in Table S3).

4.4. SDS-PAGE, Western Blot and Coomassie brilliant Analysis

After the purification, Coomassie brilliant was used to examine the purity of proteins. Purified proteins were series diluted (0, 2, 4, 8, 16, 32, 64, 128, 256 folds), and loading buffer with or without β-mercaptoethanol was incubed with purified proteins at 37°C or 100°C for 10 min. Then these sample were subjected to SDS-PAGE to determine the protein purity and oligomer. After that, 10 uM TYMS was incubated with 2 mM dUMP and 2 mM mTHF in 40 uL reaction system at 37°C, and then subjected to SDS-PAGE to confirm the active or inactive state of TYMS.

Western Blot was used to verify the protein expression, TYMS were subjected to SDS-PAGE, and then the SDS gel was washed with transfer buffer, proteins were transferred from the gel onto a nitrocellulose membrane with a constant current of 250 mA for 2 hrs. The membrane was blocked with 1% non-fat milk powder in PBST (PBS containing 0.05% (*v*/*v*) Tween-20). Mouse anti-His-tag antibody (Sigma) was used as the primary antibody at a 1:5000 dilution in blocking solution. Goat-anti-Mouse was secondary antibody (sigma) which was diluted at 1:3000, Protein bands were detected on photographic films using an enhanced chemiluminescent substrate.

4.5. Activity Detection

TYMS activity assay were carried out in 100 uL reaction volume containing reaction buffer (10 mM boracic acid pH 6.0, 150 mM NaCl), 200 uM mTHF, 1 uM dUMP, and 10 uM TYMS. After incubation at 37°C for 3 hrs, CIAP was added at a final concentration of 1 U and the reaction was incubated at 37°C for 4 hrs. The samples were then subjected to HPLC-MS/MS analysis of deoxyuridine (dU) and deoxythymidine (dT). Quantification was performed using an HPLC system (Waters) coupled to an API 5500 triple quadrupole (ABSciex) operating in positive electrospray ionization mode. The chromatographic separation was performed at 25°C with the use of C18 reverse-phase column (150 × 2.1 mm; 5 µm particle size; Thermo Fisher). The mobile phase consisted of A (water and 0.1% formic acid) and B (methanol and 0.1% formic acid) solutions [37]. The following conditions were employed during chromatography: 0.4 ml/min flow, 0-1 min, 1% B; 1- 2 min, to 20% B; 2-3 min, to 20%B, 3-4 min, 1% B. To minimize potential salt and other contaminants in the ESI

source, a time segment was set to direct the first 0.5 min of column elute to waste. For mass spectrometry detection, the multiple reaction monitoring was implemented using the following mass transitions: 243.1/127.1 (dT) and 243.1/127.1 (dU).

4.6. Size Exclusion Chromatography

Purified TYMS by Ni-NTA column was subjected to SEC at a flow rate of 1.0 mL/min on a Superdex-200 HiLoad 10/300 column (GE Healthcare) that had been prequilibrated with HEPES buffer (10 mM HEPES, 150 mM NaCl, 10% glycerol, pH7.4). The eluent is collected in constant volumes 500 μL and examined by ultraviolet absorption at 280 nm. Columns are often calibrated using 5 standard samples including myosin (212.0 kDa), beta-galactosidase (116.0 kDa), bovine serum albumin (67.0 kDa), ovalbumin (43.0 kDa), and ribonuclease A (13.7 kDa).

The components separated by SEC were concentrated using an Amicon Ultrafree centrifugal filter (Millipore Corporation, Billerica, MA, USA) with a cutoff of 10 kDa in Concentration Buffer. The dimer and octamer separated by SEC were subjected to NATIVE-PAGE (7.5%) and monomer was subjected to SDS-PAGE (12%), and then, analyzed by using Western Blot and Coomassie brilliant. For NATIVE-PAGE, Samples were run at constant voltage (100V before the indicator to spacer gel, and then, turn to 120V).

4.7. Reaction Kinetics Detection

Enzyme activity was determined by measuring the formation of dihydrofolate, which was monitored at 340 nm after addition of enzyme to the reaction assay[27, 38]. Measurements were made at pH 6.0 and 37 °C in Reaction buffer (10 mM Boric acid, 150 mM NaCl) for 5min. To determine the K_m(dUMP) for different oligomeric forms, varying concentrations of dUMP (0-50 μM) were used with constant concentrations of enzyme (0.75uM) and mTHF (100 μM). K_m(mTHF) was determined with varying concentrations of mTHF (0-100μM) were used with constant concentrations of enzyme (0.75uM) and dUMP (50 μM).

Supplementary Materials: Supplementary materials can be found at https://www.preprints.org/manuscript/201804.0014/v1.

Acknowledgments: This study was supported by grants from the National Natural Science Foundation of China (Nos. 81502622 to Lina Wang) and Natural Science Foundation of Liaoning Province (Nos. 201602239 to Lina Wang). This study was also supported by grants from the National Natural Science Foundation of China (NSFC Nos. 31471328 and 81622040 to Qingkai Yang).

Author Contributions: Author Contributions: Lina Wang and Qingkai Yang co-designed the research. Dan Xie performed most experiments and wrote the paper, Lulu Wang detected the oligomeric forms using SEC, Qi Xiao constructed the plasmids, Xiaoyan Wu, performed some western blot analysis.

Conflict of Interest: All authors declare no conflicting financial interests.

References

1. Choi, Y. M.; Yeo, H. K.; Park, Y. W.; Lee, J. Y., Structural Analysis of Thymidylate Synthase from Kaposi's Sarcoma-Associated Herpesvirus with the Anticancer Drug Raltitrexed. *PloS one* **2016,** 11, (12), e0168019.
2. Koehn, E. M.; Fleischmann, T.; Conrad, J. A.; Palfey, B. A.; Lesley, S. A.; Mathews, II; Kohen, A., An unusual mechanism of thymidylate biosynthesis in organisms containing the thyX gene. *Nature* **2009,** 458, (7240), 919-23.
3. Evans, D. R.; Guy, H. I., Mammalian pyrimidine biosynthesis: fresh insights into an ancient pathway. *The Journal of biological chemistry* **2004,** 279, (32), 33035-8.
4. Carreras, C. W.; Santi, D. V., The catalytic mechanism and structure of thymidylate synthase. *Annual review of biochemistry* **1995,** 64, 721-62.
5. Finer-Moore, J. S.; Santi, D. V.; Stroud, R. M., Lessons and conclusions from dissecting the mechanism of a bisubstrate enzyme: thymidylate synthase mutagenesis, function, and structure. *Biochemistry* **2003,** 42, (2), 248-56.

6. Myllykallio, H.; Lipowski, G.; Leduc, D.; Filee, J.; Forterre, P.; Liebl, U., An alternative flavin-dependent mechanism for thymidylate synthesis. *Science (New York, N.Y.)* **2002,** 297, (5578), 105-7.
7. Mathews, II; Deacon, A. M.; Canaves, J. M.; McMullan, D.; Lesley, S. A.; Agarwalla, S.; Kuhn, P., Functional analysis of substrate and cofactor complex structures of a thymidylate synthase-complementing protein. *Structure (London, England : 1993)* **2003,** 11, (6), 677-90.
8. Lesley, S. A.; Kuhn, P.; Godzik, A.; Deacon, A. M.; Mathews, I.; Kreusch, A.; Spraggon, G.; Klock, H. E.; McMullan, D.; Shin, T.; Vincent, J.; Robb, A.; Brinen, L. S.; Miller, M. D.; McPhillips, T. M.; Miller, M. A.; Scheibe, D.; Canaves, J. M.; Guda, C.; Jaroszewski, L.; Selby, T. L.; Elsliger, M. A.; Wooley, J.; Taylor, S. S.; Hodgson, K. O.; Wilson, I. A.; Schultz, P. G.; Stevens, R. C., Structural genomics of the Thermotoga maritima proteome implemented in a high-throughput structure determination pipeline. *Proceedings of the National Academy of Sciences of the United States of America* **2002,** 99, (18), 11664-9.
9. Leduc, D.; Graziani, S.; Meslet-Cladiere, L.; Sodolescu, A.; Liebl, U.; Myllykallio, H., Two distinct pathways for thymidylate (dTMP) synthesis in (hyper)thermophilic Bacteria and Archaea. *Biochemical Society transactions* **2004,** 32, (Pt 2), 231-5.
10. Mishanina, T. V.; Yu, L.; Karunaratne, K.; Mondal, D.; Corcoran, J. M.; Choi, M. A.; Kohen, A., An unprecedented mechanism of nucleotide methylation in organisms containing thyX. *Science (New York, N.Y.)* **2016,** 351, (6272), 507-10.
11. Papamichael, D., The use of thymidylate synthase inhibitors in the treatment of advanced colorectal cancer: current status. *Stem cells (Dayton, Ohio)* **2000,** 18, (3), 166-75.
12. Santhekadur, P. K.; Rajasekaran, D.; Siddiq, A.; Gredler, R.; Chen, D.; Schaus, S. E.; Hansen, U.; Fisher, P. B.; Sarkar, D., The transcription factor LSF: a novel oncogene for hepatocellular carcinoma. *American journal of cancer research* **2012,** 2, (3), 269-85.
13. Wilson, P. M.; Danenberg, P. V.; Johnston, P. G.; Lenz, H. J.; Ladner, R. D., Standing the test of time: targeting thymidylate biosynthesis in cancer therapy. *Nature reviews. Clinical oncology* **2014,** 11, (5), 282-98.
14. Assaraf, Y. G., Molecular basis of antifolate resistance. *Cancer metastasis reviews* **2007,** 26, (1), 153-81.
15. Wang, W.; Marsh, S.; Cassidy, J.; McLeod, H. L., Pharmacogenomic dissection of resistance to thymidylate synthase inhibitors. *Cancer research* **2001,** 61, (14), 5505-10.
16. Kitchens, M. E.; Forsthoefel, A. M.; Barbour, K. W.; Spencer, H. T.; Berger, F. G., Mechanisms of acquired resistance to thymidylate synthase inhibitors: the role of enzyme stability. *Molecular pharmacology* **1999,** 56, (5), 1063-70.
17. Phan, J.; Koli, S.; Minor, W.; Dunlap, R. B.; Berger, S. H.; Lebioda, L., Human thymidylate synthase is in the closed conformation when complexed with dUMP and raltitrexed, an antifolate drug. *Biochemistry* **2001,** 40, (7), 1897-902.
18. Genovese, F.; Ferrari, S.; Guaitoli, G.; Caselli, M.; Costi, M. P.; Ponterini, G., Dimer-monomer equilibrium of human thymidylate synthase monitored by fluorescence resonance energy transfer. *Protein science : a publication of the Protein Society* **2010,** 19, (5), 1023-30.
19. Schiffer, C. A.; Clifton, I. J.; Davisson, V. J.; Santi, D. V.; Stroud, R. M., Crystal structure of human thymidylate synthase: a structural mechanism for guiding substrates into the active site. *Biochemistry* **1995,** 34, (50), 16279-87.
20. Lin, X.; Liu, J.; Maley, F.; Chu, E., Role of cysteine amino acid residues on the RNA binding activity of human thymidylate synthase. *Nucleic acids research* **2003,** 31, (16), 4882-7.
21. Berger, S. H.; Berger, F. G.; Lebioda, L., Effects of ligand binding and conformational switching on intracellular stability of human thymidylate synthase. *Biochimica et biophysica acta* **2004,** 1696, (1), 15-22.
22. Voeller, D. M.; Zajac-Kaye, M.; Fisher, R. J.; Allegra, C. J., The identification of thymidylate synthase peptide domains located in the interface region that bind thymidylate synthase mRNA. *Biochemical and biophysical research communications* **2002,** 297, (1), 24-31.
23. Chu, E.; Voeller, D.; Koeller, D. M.; Drake, J. C.; Takimoto, C. H.; Maley, G. F.; Maley, F.; Allegra, C. J., Identification of an RNA binding site for human thymidylate synthase. *Proceedings of the National Academy of Sciences of the United States of America* **1993,** 90, (2), 517-21.
24. Chu, E.; Koeller, D. M.; Casey, J. L.; Drake, J. C.; Chabner, B. A.; Elwood, P. C.; Zinn, S.; Allegra, C. J., Autoregulation of human thymidylate synthase messenger RNA translation by thymidylate synthase. *Proceedings of the National Academy of Sciences of the United States of America* **1991,** 88, (20), 8977-81.

25. Anderson, A. C.; O'Neil, R. H.; Surti, T. S.; Stroud, R. M., Approaches to solving the rigid receptor problem by identifying a minimal set of flexible residues during ligand docking. *Chemistry & biology* **2001,** 8, (5), 445-57.
26. Costi, M. P.; Ferrari, S.; Venturelli, A.; Calo, S.; Tondi, D.; Barlocco, D., Thymidylate synthase structure, function and implication in drug discovery. *Current medicinal chemistry* **2005,** 12, (19), 2241-58.
27. Phan, J.; Mahdavian, E.; Nivens, M. C.; Minor, W.; Berger, S.; Spencer, H. T.; Dunlap, R. B.; Lebioda, L., Catalytic cysteine of thymidylate synthase is activated upon substrate binding. *Biochemistry* **2000,** 39, (23), 6969-78.
28. Almog, R.; Waddling, C. A.; Maley, F.; Maley, G. F.; Van Roey, P., Crystal structure of a deletion mutant of human thymidylate synthase Delta (7-29) and its ternary complex with Tomudex and dUMP. *Protein science : a publication of the Protein Society* **2001,** 10, (5), 988-96.
29. Phan, J.; Steadman, D. J.; Koli, S.; Ding, W. C.; Minor, W.; Dunlap, R. B.; Berger, S. H.; Lebioda, L., Structure of human thymidylate synthase suggests advantages of chemotherapy with noncompetitive inhibitors. *The Journal of biological chemistry* **2001,** 276, (17), 14170-7.
30. Wang, N.; McCammon, J. A., Substrate channeling between the human dihydrofolate reductase and thymidylate synthase. *Protein science : a publication of the Protein Society* **2016,** 25, (1), 79-86.
31. Chen, D.; Jansson, A.; Sim, D.; Larsson, A.; Nordlund, P., Structural analyses of human thymidylate synthase reveal a site that may control conformational switching between active and inactive states. *The Journal of biological chemistry* **2017,** 292, (32), 13449-13458.
32. Salo-Ahen, O. M.; Tochowicz, A.; Pozzi, C.; Cardinale, D.; Ferrari, S.; Boum, Y.; Mangani, S.; Stroud, R. M.; Saxena, P.; Myllykallio, H.; Costi, M. P.; Ponterini, G.; Wade, R. C., Hotspots in an obligate homodimeric anticancer target. Structural and functional effects of interfacial mutations in human thymidylate synthase. *Journal of medicinal chemistry* **2015,** 58, (8), 3572-81.
33. Cella, R.; Carbonera, D.; Orsi, R.; Ferri, G.; Iadarola, P., Proteolytic and partial sequencing studies of the bifunctional dihydrofolate reductase-thymidylate synthase from Daucus carota. *Plant molecular biology* **1991,** 16, (6), 975-82.
34. Dowiercial, A.; Wilk, P.; Rypniewski, W.; Rode, W.; Jarmula, A., Crystal structure of mouse thymidylate synthase in tertiary complex with dUMP and raltitrexed reveals N-terminus architecture and two different active site conformations. *BioMed research international* **2014,** 2014, 945803.
35. Cha-Aim, K.; Hoshida, H.; Fukunaga, T.; Akada, R., Fusion PCR via novel overlap sequences. *Methods in molecular biology (Clifton, N.J.)* **2012,** 852, 97-110.
36. Wang, L.; Quan, C.; Liu, B.; Xu, Y.; Zhao, P.; Xiong, W.; Fan, S., Green fluorescent protein (GFP)-based overexpression screening and characterization of AgrC, a Receptor protein of quorum sensing in Staphylococcus aureus. *International journal of molecular sciences* **2013,** 14, (9), 18470-87.
37. Zhu, Y.; Zhou, G.; Yu, X.; Xu, Q.; Wang, K.; Xie, D.; Yang, Q.; Wang, L., LC-MS-MS quantitative analysis reveals the association between FTO and DNA methylation. *PloS one* **2017,** 12, (4), e0175849.
38. Dunlap, R. B.; Harding, N. G.; Huennekens, F. M., Thymidylate synthetase from amethopterin-resistant Lactobacillus casei. *Biochemistry* **1971,** 10, (1), 88-97.